Solar Physics (2023) 298:68
https://doi.org/10.1007/s11207-023-02166-x

RESEARCH

The *Advanced Space-Based Solar Observatory* (ASO-S)

Weiqun Gan[1] · Cheng Zhu[2] · Yuanyong Deng[3] · Zhe Zhang[1] · Bo Chen[4] · Yu Huang[1] · Lei Deng[2] · Haiyan Wu[5] · Haiying Zhang[6] · Hui Li[1] · Yang Su[1] · Jiangtao Su[3] · Li Feng[1] · Jian Wu[1] · Jijun Cui[5] · Chi Wang[5] · Jin Chang[1] · Zengshan Yin[2] · Weiming Xiong[5] · Bin Chen[5] · Jianfeng Yang[7] · Fu Li[7] · Jiaben Lin[3] · Junfeng Hou[3] · Xianyong Bai[3] · Dengyi Chen[1] · Yan Zhang[1] · Yiming Hu[1] · Yaoming Liang[5] · Jianping Wang[2] · Kefei Song[4] · Quanfeng Guo[4] · Lingping He[4] · Guang Zhang[4] · Peng Wang[4] · Haicao Bao[2] · Caixia Cao[2] · Yanping Bai[2] · Binglong Chen[2] · Tao He[2] · Xinyu Li[2] · Ye Zhang[2] · Xing Liao[2] · Hu Jiang[2] · Youping Li[1] · Yingna Su[1] · Shijun Lei[1] · Wei Chen[1] · Ying Li[1] · Jie Zhao[1] · Jingwei Li[1] · Yunyi Ge[1] · Ziming Zou[5] · Tai Hu[5] · Miao Su[5] · Haidong Ji[8] · Mei Gu[9] · Yonghuang Zheng[10] · Dezhen Xu[11] · Xing Wang[12]

Received: 27 January 2023 / Accepted: 13 May 2023 / Published online: 24 May 2023

Abstract
The *Advanced Space-based Solar Observatory* (ASO-S) was successfully launched at 23:43 UT on 8 October 2022. Here we describe the final technical status of the whole mission right before the launch, including the spacecraft platform and the three onboard payloads. The mission's science goals, organizations, preliminary performance in the commissioning phase, and the first-light results of the three payloads are briefly presented.

1. Introduction

The *Advanced Space-based Solar Observatory* (ASO-S, Chinese nickname *Kuafu*-1), the first comprehensive Chinese dedicated solar observatory in space (Gan et al., 2019a,c; Gan, Feng, and Su, 2022; Gan et al., 2019b), was successfully launched by a LM-2D rocket at 23:43 UT on 8 October 2022 from the Jiuquan Satellite Launch Center, Gansu Province, China. ASO-S was supported within the framework of the newly established Strategic Priority Program on Space Science of the Chinese Academy of Sciences (CAS), and underwent a conceptual study (2011 – 2013), background study (2014 – 2016), and comprehensive evaluation (2016 – 2017). At the end of 2017, ASO-S was formally approved by the CAS. Since then, ASO-S entered into the engineering phases via the official Phase-B (January 2018 – April 2019), Phase-C (May 2019 – August 2021), and Phase-D (September 2021 – September 2022).

The primary scientific objectives of the ASO-S can be simply expressed by "1M2B", where M stands for solar magnetic field and 2B for the two most violent eruptions on the Sun – solar flares and coronal mass ejections (CMEs), that is to observe and study their formation, evolution, interaction, and mutual relevance. Specifically, the three relationships between solar magnetic field and solar flares, solar flares and CMEs, and CMEs and solar magnetic field are the focus of attention for ASO-S. To realize these scientific goals, ASO-S

Extended author information available on the last page of the article

Table 1 Organization of ASO-S mission.

Mission level	
Chief Scientist	Weiqun Gan (Purple Mountain Observatory: PMO)
Chief Designer	Jijun Cui (National Space Science Center: NSSC)
Chief Administrator	Chi Wang (NSSC)
Principal investigators	
Spacecraft	Cheng Zhu, Lei Deng, Haicao Bao, Caixia Cao (Innovation Academy for Microsatellites: Microsat)
FMG	Yuanyong Deng (National Astronomical Observatories: NAOC), Haiying Zhang (Nanjing Institute of Astronomical Optics & Technology: NIAOT), Jianfeng Yang (Xi'an Institute of Optics and Precision Mechanics: XIOPM), Jiangtao Su (NAOC)
HXI	Zhe Zhang, Yang Su, Jian Wu (PMO)
LST	Bo Chen (Changchun Institute of Optics, Fine Mechanics and Physics: CIOMP), Hui Li, Li Feng (PMO)
SMOC	Ziming Zou, Haiyan Wu, Tai Hu (NSSC)
SODC	Hui Li, Yu Huang, Youping Li (PMO)

employs three payloads: the *Full disc vector MagnetoGraph* (FMG), for measuring the full-disk solar vector magnetic field; the *Hard X-ray Imager* (HXI), for observing non-thermal signals from ≈ 30 to 200 keV emitted by energetic electrons; and the *Lyman-α Solar Telescope* (LST), for observing both the solar disk and inner corona up to 2.5 solar radii in Lyman-α and visible light. The characteristics of the mission, beside the exclusive scientific objectives of "1M2B" and therefore the unique deployment of the payloads, also include a single near-Earth-orbit platform to perform simultaneous observations of full-disc solar vector magnetic field, nonthermal hard X-ray spectral imaging, and the formation as well as the propagation of CMEs from the disc to the nearby corona in dual wavebands. Each payload has its own special features. For instance, FMG balances both high sensitivity and high temporal resolution; HXI obtains accurate flux and more spatial-modulation Fourier components than a similar instrument before such as *Hard X-ray Telescope* onboard *Yohkoh* (Kosugi et al., 1991), and LST will take seamless observations in Lyman-α waveband from the disk center to 2.5 solar radii for the first time. Some comparisons between the ASO-S payload and other missions' payloads were made by Gan et al. (2015). The organization of the mission is briefly listed in Table 1.

The early introductory publications related to ASO-S until the end of Phase-B were collected by Gan et al. (2019b). Here we provide the status of the mission since then and the final parameters just before the launch, briefly mention the in-flight performance, present roughly a part of the first light of the payloads, and discuss briefly the scientific return and plans in the near future.

2. Spacecraft

The architecture of the ASO-S is composed of two modules: platform module and payload module. The platform module contains various of instruments belonging to seven different subsystems of the spacecraft (SC). The payload module contains the three payloads. The two modules are designed such that multiple instruments from different payloads can work most tranquilly and stably. That is to say, the state-of-the-art fabrication of the SC makes it

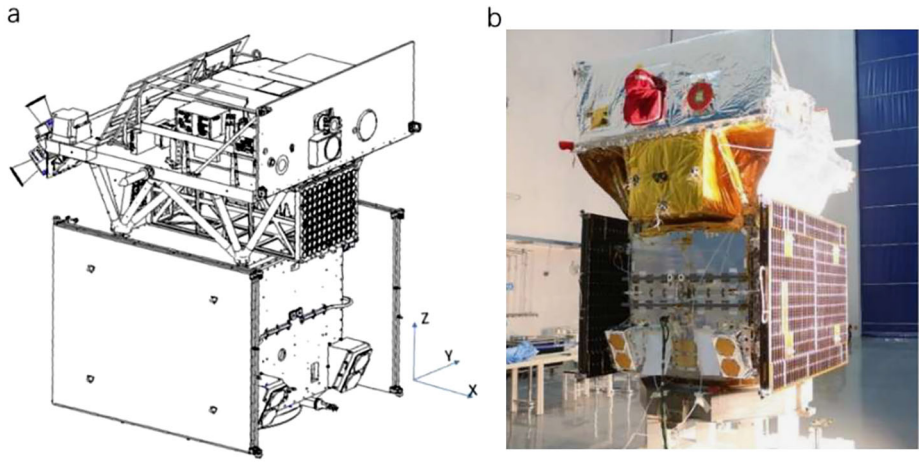

Figure 1 ASO-S designed (**a**) and actual configuration before the launch (**b**). The envelope is 1953 mm × 9184 mm × 2450 mm in the X-, Y-, and Z-dimensions.

possible for little vibration influence on the payload functioning due to oscillation sources from solar arrays and attitude controlling, for example.

The attitude–orbit control subsystem (AOCS) includes attitude-sensing devices such as the star tracker, gyroscope, Sun sensors, and attitude actuators such as momentum wheels, magnetic-torque device, and magnetometer. The effective combination of attitude devices and innovative algorithms of the AOCS contributes to a good performance: the pointing accuracy is better than $36''$ (3σ), and the pointing stability is better than $1.8''$ s^{-1} (3σ). Such attitude specifics can meet the requirements of efficient payload observations, together with the self-carried stability subsystem of the payloads. Another feature of the SC is that phased arrays of antennas are introduced for data transmission, which make the data transmission both efficient and the state of the art. The SC has two solar arrays deployed along the +Y-axis and −Y-axis in satellite-body fixed coordinates (cf. Figure 1). The envelope of the SC is 1953 mm × 9184 mm × 2450 mm in X-, Y-, Z-dimensions when it flies freely in space. The SC mass is about 857 kg. Its main working attitude is Sun pointing. The X-axis of the spacecraft body fixed coordinate system is along the Sun direction, and the Z-axis parallel to the normal of Earth's ecliptic plane.

The SC is now in a Sun-synchronous orbit with an altitude of about 720 km above the Earth's surface, and the descending node time is at 0600 local time. Such an orbit makes it more efficient to observe the Sun, although it causes some eclipse in each orbit from May to August, and the maximum eclipse time is 18 minutes. The atmosphere at an altitude of 720 km is so sparse that it will not shorten the lifespan of SC. The design lifespan is not less than four years. The final specifications for the ASO-S are listed in Table 2. The designed and actual configuration before the launch are shown in Figure 1.

3. Payloads

The design and test results of the payload engineering model (EM or phase-B study) have been introduced in detail (Deng et al., 2019; Li et al., 2019; Chen et al., 2019; Zhang et al., 2019a,b). Here, we mainly present the updated information after EM, including the technical

Table 2 Specifications of the ASO-S spacecraft.

Items		Specifications
Orbit	Orbit type	Sun-synchronous
	Altitude	720 ± 5 km
	Inclination	98.27°
	Eccentricity	0
	Local time for SC passing the descending node	0600 local
Attitude	Pointing	Sun pointing three-axis stabilized
	Accuracy	better than $36''$ (3σ)
	Stability	better than $1.8''$ s^{-1} (3σ)
SC size	Envelope before launch	$\leq \varphi$ 2900 mm × 2760 mm
Timing of SC	Timing accuracy	≤ 5 ms
Data transmission and storage	Data transmission	X band, transmission rate $\geq$ 1000 Mbps
	Allowed data storage	≥ 4 Tbits
Energy	Solar array	GaAs cell, solar array area ≥ 6 m^2
	Battery	Li battery pack $\geq$90 Ah
TT&C (Tracking,Telemetry and Control)	Data rate	S band upload rate: 2000 bps, download data rate: 8192 bps
	Orbit determination accuracy	better than 50 m (1σ)
Power	Average power consumption	$\leq$ 980 W
	Peak power consumption	$\leq$ 1417 W
Mass	Total mass	857 kg
Lifespan	Design lifespan	≥ 4 years
Reliability	Reliability	≥ 0.6 (at the end of nominal lifespan)

status change in the later qualification model (QM) and the flight model (FM), as well as some test results.

3.1. FMG

FMG is a birefringent-filter-based magnetograph, aiming to measure the photospheric magnetic fields of the entire solar disk with high spatial and temporal resolution, and high magnetic sensitivity. Most of the technical status of QM and FM are consistent with the EM (Deng et al., 2019; Su et al., 2019a), except the *Image Detecting System* (IDS) in the *Data Acquisition, Processing and Control System* (DAPCS) panel. We use another kind of CMOS sensor, named KP1010, in the QM and FM. The total array of KP1010 is 10k × 10k, the size of a single pixel is 6.4 μm. In our application, we use just 8k × 8k pixels in its central part. After exposure, we first carry out 2 × 2 binning onboard and then output 4k × 4k image. The performance of the KP1010 (after 2 × 2 binning) is listed in Table 3.

Table 3 Main performance specifics for the FM of FMG.

Items	Measurements
FOV	$33.67'$
Spatial resolution	$1.04''$
FWHM of Birefringent (BF) filter (@ 532.42 nm)	0.01014 nm
Stability of the BF passband	0.0016 nm
Out of band suppression of BF	13.0%
Sensitivity of polarization measurement	2650:1 @ 1080 s (deep integration mode)
	1020:1 @ 120 s (routine observation mode)
Max frame rate of KP1010 (after 2 × 2 binning)	10 fps
Full well capacity of KP1010	42,310 e^-
Photo response non-uniformity of KP1010	0.64%
Readout noise of KP1010	25.38 e^- $pixel^{-1}$
Onboard data-processing capability of the DAPCS	16.13 fps
Response time for polarization analyzer	≤ 50 ms
Adjusting range of pointing	Y: $\pm 2.5'$, Z: $\pm 1.75'$
Accuracy of image stabilization	$\leq 0.25''$ (1σ) per 30 s

We conducted the test observations with the QM from 25 July to 14 August 2020 at the Huairou Solar Observing Station (HSOS), NAOC. The main purpose of this test observation was to evaluate the performance of the magnetic-field measurement, as we have changed the most important unit, the image sensor in QM and FM, and to evaluate the other performances. We carried out the polarization measurement at -0.008 nm from the center of the Fe I 532.19 nm line. In the "routine observation" mode, we collected left- and right-polarization images alternately, which was repeated 128 times to deduce the Stokes-V signal, and further got the longitudinal magnetogram after calibration. The "deep integration" mode will be realized by repeating 9 times the "routine observation", and it takes about 18 minutes. Figure 2 shows a filtergram (Panel a) and corresponding longitudinal magnetogram (Panel b) of the "deep integration" mode. The magnetic sensitivity is estimated by a "quiet" region near the disk center. We use the standard deviation of this "quiet" region as the sensitivity for magnetic field, which is about 5.2 Gauss and 2.5 Gauss, in "routine observation" mode and "deep integration" mode, respectively.

The FM was only tested in the laboratory. There are two reasons why we did not carry out test observations. On the one hand, it is difficult to ensure that the instrument would not be contaminated during the trial observation; on the other hand, the focal plane of FM is designed according to the vacuum wavelength, and there would be no clear image on the camera in the air. Figure 3 shows the FM of FMG, and Table 3 lists the main performance measured for the final FMG, which satisfy well the designed requirements.

3.2. HXI

HXI is a Fourier-transform-type X-ray indirect-imaging telescope aiming to explore the nonthermal radiation process of solar flares. It is designed to image the full solar disk in the energy range of 30 – 200 keV with a spatial resolution of better than $3.2''$ at 30 keV. The design and verification of the EM and QM of HXI can be retrieved in a series of articles (Zhang et al., 2019a,b; Su et al., 2019b; Chen et al., 2020, 2021). In short, HXI includes three main

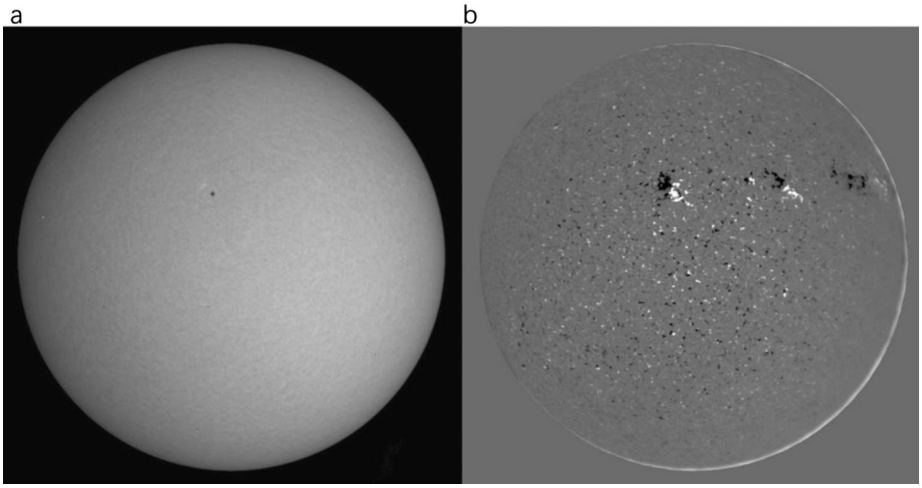

Figure 2 FMG test observations with the QM: a filtergram of Fe I 5324.185 Å (**a**) and corresponding longitudinal magnetogram (**b**).

Figure 3 The flight model of FMG (dimension: 1510 mm × 636 mm × 350 mm).

parts: the *collimator* (HXI-C), the *spectrometer* (HXI-S), and the *electronics control box* (HXI-E), which are mainly used for X-ray flux modulation, modulated X-ray photon detection, and operation management, respectively. Ninety-one pairs of tungsten grids, namely sub-collimators, modulate the incident X-ray flux simultaneously with a series of spatial frequencies. Moreover, a *solar aspect system* (SAS) attached to the HXI-C is employed to monitor the deformation of HXI-C and resolve the solar aspect information.

The FM of HXI, as shown in Figure 4, had been produced and tested during 2020 and 2021 (Wan et al., 2022; Liu et al., 2022). Its design is almost the same as that of the EM and QM on the basis of good and reliable preliminary work. At the very beginning of 2022, the FM of HXI was delivered to Microsat in Shanghai for assembly, integration, and testing with the spacecraft before launch. Some major performance specifications for the FM of HXI had been finally measured during these tests, which are listed in Table 4.

For the FM of HXI, we only mention briefly the work on the deformation monitoring of HXI-C and the X-ray beam test. The deformation of HXI-C, including relative shift and rotation between front and rear grids, has a serious impact on the imaging performance of HXI. Therefore, the deformation is carefully monitored during each test or transportation

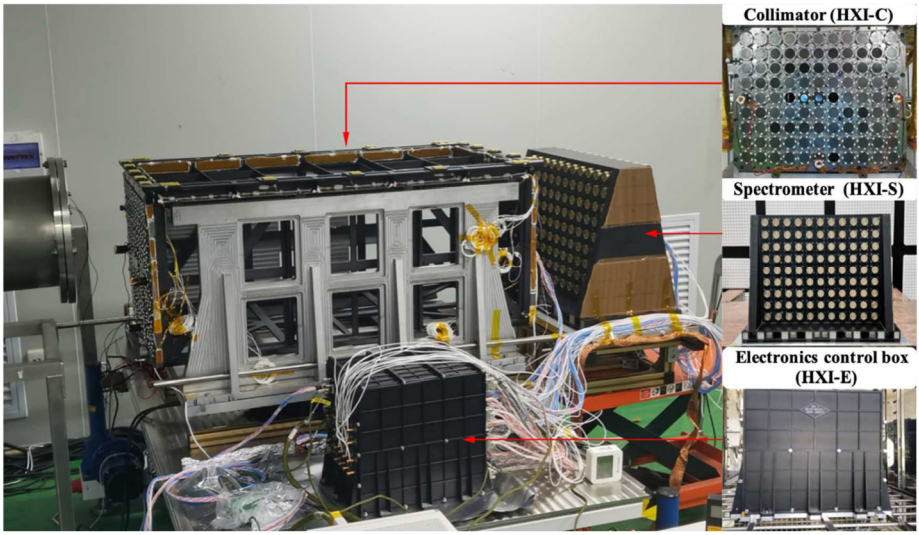

Figure 4 The flight model of HXI, running in the beam test. The dimensions for HXI-C and HXI-S are 708 mm × 700 mm × 1618 mm and for HXI-E 406 mm × 296 mm × 339 mm.

Table 4 Main performance specifications for the FM of HXI.

Items	Measurements
Energy range	30 keV to 200 keV for imaging, better than 30 keV to 400 keV for spectrum
Energy resolution (FWHM)	$< 23.7\%$ @ 32 keV
Spatial resolution	$3.2''$ @ 30 keV
Temporal resolution	0.125 s, 0.25 s, 0.5 s, and 1 s for eruption periods, 4 s for quiet periods
FOV	Full Sun, $40.3'$
Pointing precision of SAS	$0.63''$ for the Sun center
Deformation of the collimator	relative rotation $< 5.7''$ and relative shift < 18.4 μm before launch
Deadtime for detectors	≈ 1.8 μs
Gain difference between detectors	$< 16.2\%$
Updating frequency for SAS dataset	4 Hz

accomplished in the whole period from assembly to launch. The SAS was used as the only measurement method to monitor the deformation since the HXI-C was integrated into the spacecraft. The other methods, such as the coordinate-measuring machine, are no longer suitable due to interference with the spacecraft. The FM of HXI-C maintained good stability during the whole period according to the monitoring results that the relative shift varies less than 18.4 μm and relative rotation less than $5.7''$. These values are much better than the design specifications, which were required to keep less than 30 μm for shift and $10''$ for rotation before launch. On the other hand, knowledge about the X-ray flux modulation relation of each sub-collimator is considered as the basis of modulation imaging of HXI. For this reason, an X-ray beam test is employed to directly verify and calibrate the modulation

relation of the FM of HXI-C on a dedicated X-ray beam facility. The modulation relation curves of all 91 grid pairs of the FM, including the finest ones with a pitch of 36 μm, have been obtained by the beam test lasting more than one month on the facility. The high-quality results prove the reliability of the modulation imaging system and could be used as imaging parameters for image reconstruction of observations on orbit.

3.3. LST

LST is the first Chinese space telescope to observe the Sun from disk center to the inner corona up to 2.5 $R_\odot$ in both the Lyman-α and white-light wavebands (cf. Table 5) for diverse solar activities and the quiet Sun. The scientific objectives of LST and its contributions to the main objectives of the ASO-S have been extensively described in previous articles (Li et al., 2019; Feng et al., 2019). LST is a suite of imaging instruments, including the *Solar Corona Imager* (SCI), which is a Lyot-type coronagraph working in both the Lyman-α and 700 nm wavebands (called SCIUV and SCIWL, respectively), the *Solar Disk Imager* (SDI), and the *White-light Solar Telescope* (WST) working in the Lyman-α and 360 nm waveband, respectively (see Table 5 for specific information). SCIUV and SCIWL share the same optical design, and a beam-splitter is used to reflect Lyman-α and transmit the 700 nm waveband. Each of the four instruments of LST has its default observation modes/cadences, which have been described in detail in previous articles (Li et al., 2019; Feng et al., 2019). The EM's optical, mechanical, electrical, and thermal designs have been presented in detail (Chen et al., 2019). The stabilization capability of the spacecraft does not satisfy the requirement of SDI and SCI images. To meet the stringent requirement, the SCI primary mirror is an active mirror driven by a piezoelectric table, which tracks the Sun according to the pointing signal from the *guide telescope* (GT) of the LST and has an angular compensation of $\pm 214''$. The secondary mirror of SDI is also an active mirror and has an angular compensation of $\pm 69''$. The SCI, the SDI, and the WST share a common mechanical bench with sufficient stability and stiffness to retain their optical axes consistency within $\pm 10''$. After the EM of the LST, some changes and updates have been made to optimize the parameters and improve the characteristics and performance. Here we briefly report on several major ones.

In order to achieve the stringent requirement for stray-light suppression of the SCI, a gradient coating is deposited on the SCI's secondary-mirror inner edge, which smoothly decreases reflectivity from 1.3 $R_\odot$ to 1.1 $R_\odot$ region for the white-light waveband while that for the Lyman-α waveband is almost unchanged. Meanwhile, the Lyot stop also plays an important role in stray-light suppression by reducing the effective aperture to about 48 mm, which is an appropriate size instead of the 60 mm clear aperture of the main mirror. Compared with the EM, another Lyman-α filter was added near the entrance of the SDI to improve the spectral purity. Therefore, in the QM and FM, the SDI has two pre-filters at the entrance and one filter on the filter wheel. Calculations show that this combination reduces the out-of-band radiation down to around 2%. In order to improve the in-flight flat-field calibration accuracy by the KLL algorithm (Kuhn, Lin, and Loranz, 1991), a defocusing lens is added in the front of SDI's CMOS detector (on the filter wheel) to blur the apparent structures of the solar disk in the observing waveband so that the acquired images are more suitable for the KLL algorithm (Li et al., 2021).

Before launch, all on-ground tests, measurements, and calibrations of LST have been done at CIOMP. Figure 5 shows an FM photo of LST. The main test and calibration results are shown in Table 5. The center wavelengths and bandwidths (FWHM) of the four instruments in Table 5 were derived from the spectral response curves obtained on-ground before launch.

Table 5 Main test and measured parameters for the FM of LST.

Items	Instruments	Measurements
Center wavelength	SCI	701.0 nm and 122.6 nm
	SDI	121.6 nm
	WST	360.0 nm
Bandwidth (FWHM)	SCI	62.7 nm @ 700.0 nm, 6.0 nm @ 121.6 nm
	SDI	9.5 nm
	WST	3.7 nm
FOV	SCI	Inner 33.7′, Outer 80.2′ @ 700.0 nm
		Inner 33.7′, Outer 80.6′ @ 121.6 nm
	SDI	38.5′
	WST	38.7′
Spatial resolution	SCI	4.4″
	SDI	1.2″
	WST	1.1″
Image stabilization (1σ)	SCI	0.2″ per 120 s
	SDI	0.1″ per 60 s
Stray-light suppression (700 nm)	SCI	1.5×10^{-7} $B_\odot$ @ 1.1 $R_\odot$, 3.5×10^{-8} $B_\odot$ @ 2.5 $R_\odot$
Scope for image stabilization	SCI	±214″
	SDI	±69″

Figure 5 The flight model of LST (dimensions: 1380 mm × 818 mm × 474 mm).

4. Operation

For most of the commissioning time and later normal working time, both the *Space Science Mission Operation Center* (SMOC) at NSSC, CAS and the ASO-S *Science Operation and Data Center* (SODC) (Huang et al., 2019) at PMO, CAS are together responsible for managing the spacecraft in orbit. The original data are transferred to SMOC from three ground stations located at Sanya, Kashi, and Miyun. These three ground stations can provide the download of all of the data observed daily. Every day, there are six to nine contacts between the spacecraft and ground stations. The maximum data latency to the ground station is about ten hours. After decoding and pre-processing, the data are transferred from SMOC to the SODC, where they are processed further into high-level data, which are stored and will be open, together with analysis software, to users all over the world afterwards.

After the commissioning phase, the mission will work automatically for most of the time, but there are indeed different modes, which can be commanded from the ground or adjusted autonomously through detection software running onboard, for the former, for example, from routine (two-minute cadence) to deep integration mode for FMG; for the latter, for example, the eruption mode or quiet mode for HXI. In order to satisfy specific campaigns or specific goals, SODC can upload one day ahead a series of commands.

At the time of writing (three months since launch), the mission works well and various commissioning-phase tests are being done step-by-step. We plan to finish all commissioning tests and in-flight calibrations within six months, and then we will open all the data to the community in real time via the SODC data access at the mission home page at aso-s.pmo.ac.cn/en_index.jsp. Before that time, the ASO-S science team plans to hold a training course (most probably via online meetings) to teach users how to access and analyze the data.[1] The data policy of the ASO-S was made by the science committee over two years ago, in which it emphasizes the equal right for users or the team members to access the scientific data of the ASO-S mission, encouraging collaboration with team members for the initial two years, and beyond. The full version of the data policy can be referred to at the home page of the ASO-S mission.

The ASO-S science team has the duty to organize and promote the research based on the ASO-S data. Beside focused projects supporting analyzing the ASO-S data in China, the ASO-S science team also plans to issue an international cooperation program in due time, in which over ten guest investigators are annually invited to visit SODC for a couple of months to perform joint or independent research related to ASO-S data. The regular ASO-S international workshop or a joint workshop with other missions are being considered, depending on the performance of the mission. We hope indeed that with a rich scientific return, the ASO-S could make a remarkable contribution to the solar studies in Solar Cycle 25.

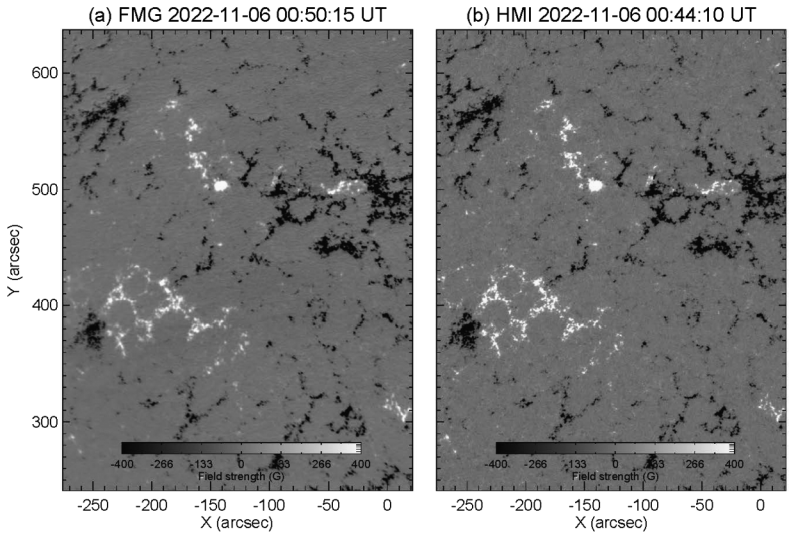

Figure 6 Line-of-sight magnetogram in quiet Sun acquired by FMG on 06 November 2022 00:50:15 UT (**a**) and the corresponding HMI magnetogram (**b**) is shown for comparison.

[1] At the time that this article was accepted for publication, the tutorial on ASO-S data had already been held from 11 to 12 April 2023 online. All the materials of the tutorial have been put on the website of the mission.

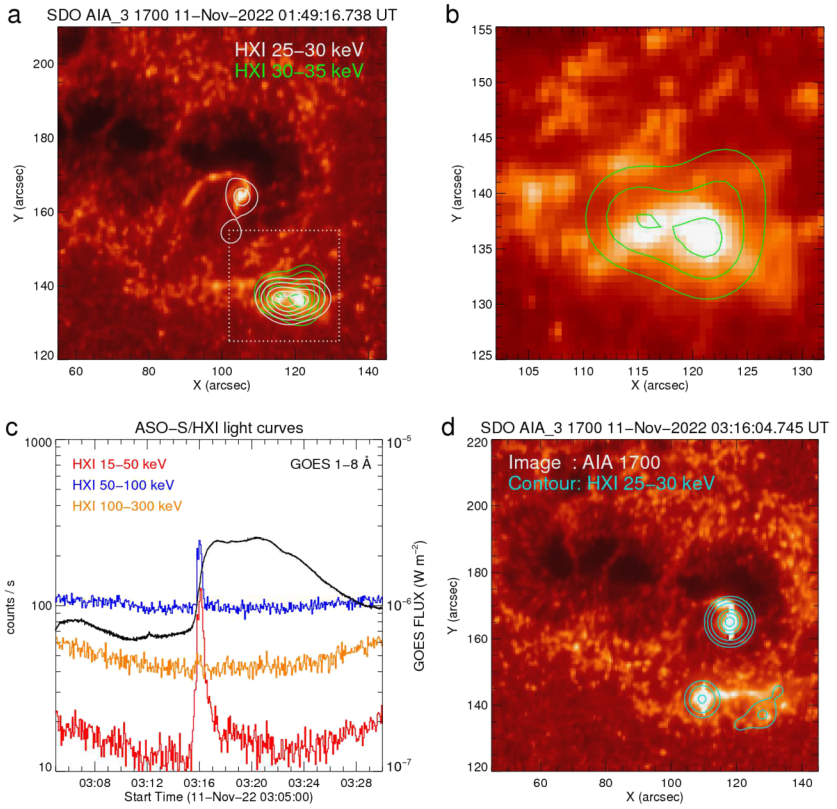

Figure 7 HXI/ASO-S X-ray light curves and images of two flares observed on 11 November 2022. (**a**) The HXI/ASO-S images reconstructed using the HXI Clean algorithm (Su et al., 2019) in the energy ranges of 25 – 30 (*white*) and 30 – 35 keV (*green*) with contour levels of 15, 30, 50, 70, and 90 percent of the peak intensity for the flare that occurred at 01:48 UT. The background 1700 Å image was taken by SDO/AIA at 01:49:16 UT. (**b**) Enlarged view of the southern ribbon with HXI 30 – 35 keV contours (30, 60, and 90 percent contours). (**c**) ASO-S/HXI light curves in the energy ranges of 15 – 50, 50 – 100, and 100 – 300 keV and GOES 1 – 8 Å light curve for the GOES C3 flare with a start time at ≈ 03:13 UT. (**d**) The ASO-S/HXI Clean image for the energy range of 25 – 30 keV (*cyan* contours at levels of 5, 10, 20, 50, 70 and 90 percent of the peak intensity). The background 1700 Å image was taken by SDO/AIA at 03:16:04 UT.

5. First Light

During the first three months since launch, the first light of the three payloads (except for SCI) have been obtained, although more elaborate calibrations are still needed.

Figure 6a shows a cutout longitudinal magnetogram of FMG in quiet Sun taken at 00:50 UT on 06 November 2022, in comparison with that observed by the *Helioseismic and Magnetic Imager* (HMI: Scherrer et al., 2012) onboard the *Solar Dynamics Observatory* (SDO: Pesnell, Thompson, and Chamberlin, 2012), as shown in Figure 6b. The FMG transverse fields as well as the full-disc magnetograms are still under test.[2]

[2]At the time that this article was accepted for publication, the FMG transverse fields have not yet been obtained. The possible reason is attributed to the performance of one of the two liquid crystal variable retarders.

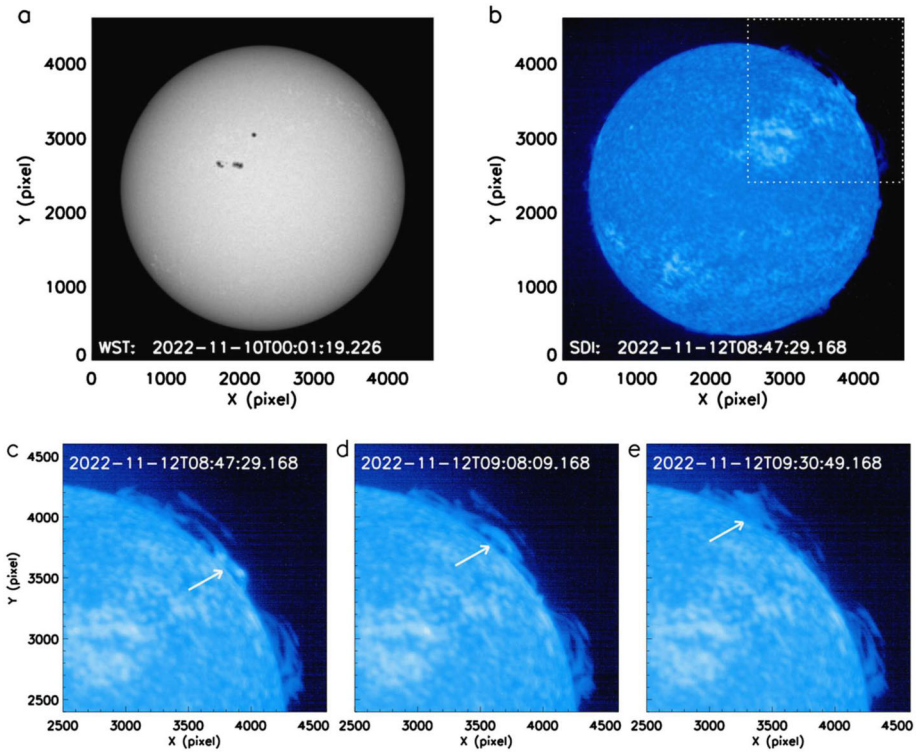

Figure 8 Panels **a** and **b**: WST and SDI full-disk images at 360 nm and 121.6 nm. The images are calibrated with in-flight dark-current and flat-field data. Panels **c** – **e**: enlargement of a subregion marked by the *dotted lines* in Panel **b** to show the fine structures of prominences and the northward plasma flows indicated by *three arrows*.

Figure 7 shows HXI CLEAN images reconstructed for a GOES C4 flare that started at 01:45 UT and the GOES C3 flare that started at 03:10 UT on 11 November 2022, overlaid on the image at 1700 Å taken by the *Atmospheric Imaging Assembly* (AIA: Lemen et al., 2012). The HXI images have been rotated so that the solar North is pointing up and corrected for the pointing shifts during the image duration. A manual shift of $\approx 91''$ (the shift will not be necessary after the full imaging calibration in the future, which requires more observations of flares) was then applied to the images to match the HXR sources with the bright ribbons seen by AIA. It is revealed that the two hard X-ray sources in the energy range of 25 – 30 keV are well consistent with the bright ribbons in the 1700 Å image (Figure 7a, d). At higher energies of 30 – 35 keV (Figure 7b), the fine structures of the two separate bright features in the southern ribbon are resolved as two sources, which suggests a correct reconstruction of HXI images at its finest resolution of $3.2''$, even though the sub-collimators are not calibrated yet.

Figure 8 demonstrates the imaging capability of WST and SDI of the LST. Panels a – b show the full-disk images of WST and SDI, respectively. In the WST image, sunspot umbra, penumbra, and light bridges can be distinguished. The SDI captures various structures on

Besides, there is a darker region in the whole-disc image. The reason and remedy are still under investigation. The details will be described in an upcoming article specifically for the instrument.

the Sun, from omnipresent chromospheric network, active regions on the disk, to the off-limb prominences. To show the fine structures of the prominences, the dotted subregion in Panel b is enlarged. The northward plasma flows indicated by three arrows can be observed, as shown in Panels c – e. At the time of this article, the SCI is still under test.[3]

The details of each instrument's performance in orbit and quality of the images will be discussed later in separate articles by each of payloads when the commissioning phase is finished. At this moment, three months since launch, the spacecraft platform is normal, and the HXI is close to finishing its tests, while FMG and LST are still under test.

Acknowledgments The ASO-S mission is a large scientific project and has lasted over ten years from the early concept study. Hundreds of people have been involved in the project for different periods of the time. All the participants are heartfeltly acknowledged! SDO is the first mission under NASA's Living With a Star (LWS) program. The SDO/AIA and SDO/HMI data used in this article were downloaded from the JSOC data center and they are courtesy of NASA and the science teams.

Author contributions Beside the contributors listed in Table 1, the contributors on the mission-level coordination include also W. Xiong, Bin Chen, and M. Su; on the spacecraft platform Z. Yin, H. Bao, C. Cao., Y. Bai, Binglong Chen, T. He, X. Li, Ye Zhang, X. Liao, and H. Jiang; on the FMG F. Li, J. Lin, J. Hou, and X. Bai; on the HXI D. Chen, Yan Zhang, Y. Hu, Y. Liang, and J. Wang; on the LST K. Song, Q. Guo, L. He, G. Zhang, and P. Wang; on the SODC Yingna Su, S. Lei, W. Chen, Ying Li, J. Zhao, J. Li, and Y. Ge; on the missions' other systems H. Ji, M. Gu, Y. Zheng, D. Xu, and X. Wang. The manuscript was organized by W. Gan with the help from all authors.

Funding The ASO-S is supported by the Strategic Priority Research Program on Space Science, Chinese Academy of Sciences (Grant No. XDA15320000, XDA15320100, XDA15320102, XDA15320103, XDA15320104, XDA15320300, XDA15052200). Part of members' own work is also supported by the Ministry of Science and Technology of China (Grant No. 2022YFF0503000), the National Natural Science Foundation of China (Grant No. 12233012, 12022302, 12173100, 11921003, U1731241, 11973097), and the Youth Innovation Promotion Association CAS.

Declarations

Competing interests The authors declare no competing interests.

References

Chen, B., Li, H., Song, K.F., Guo, Q.F., Zhang, P.J., He, L.P., et al.: 2019, The Lyman-alpha Solar Telescope (LST) for the ASO-S mission—II. Design of LST. *Res. Astron. Astrophys.* **19**, 159. DOI. ADS.

Chen, D.Y., Hu, Y.M., Zhang, Z., Zhang, Y., Zhang, Y.Q., Huang, Y., Ma, T., Chang, J.: 2020, Environmental tests of the HXI spectrometer for the ASO-S mission. *J. Instrum.* **15**, T10008. DOI. ADS.

Chen, D.Y., Hu, Y.M., Ma, T., Su, Y., Yang, J.F., Wang, J.P., et al.: 2021, Design and verification of the HXI collimator on the ASO-S mission. *Res. Astron. Astrophys.* **21**, 136. DOI. ADS.

Deng, Y.Y., Zhang, H.Y., Yang, J.F., Li, F., Lin, J.B., Hou, J.F., et al.: 2019, Design of the full-disk Magneto-Graph (FMG) onboard the ASO-S. *Res. Astron. Astrophys.* **19**, 157. DOI. ADS.

Feng, L., Li, H., Chen, B., Li, Y., Susino, R., Huang, Y., et al.: 2019, The Lyman-alpha Solar Telescope (LST) for the ASO-S mission—III. Data and potential diagnostics. *Res. Astron. Astrophys.* **19**, 162. DOI. ADS.

Gan, W.Q., Feng, L., Su, Y.: 2022, A Chinese solar observatory in space. *Nat. Astron.* **6**, 165. DOI. ADS.

Gan, W.Q., Deng, Y.Y., Li, H., Wu, J., Zhang, H.Y., Chang, J., et al.: 2015, ASO-S: Advanced Space-based Solar Observatory. *Proc. SPIE* **9604**, 96040T. DOI.

[3] At the time that this article was accepted for publication, the SCI was found to have a defect in technological design. So far, coronal structures are almost unrecognizable in 700 nm images from SCIWL, while the Lyman-α images from SCIUV look better except for some obscuration. We are still optimizing the observation parameters and modes to improve the image quality. The details will be described in an upcoming article specifically for the instrument.

Gan, W.Q., Ding, M.D., Huang, Y., Su, Y.N.: 2019a, Preface: Advanced Space-based Solar Observatory (ASO-S). *Res. Astron. Astrophys.* **19**, 155. DOI. ADS.
Gan, W.Q., Ding, M.D., Huang, Y., Su, Y.N. (eds.): 2019b, Advanced Space-based Solar Observatory (ASO-S). *Res. Astron. Astrophys.* **19**. URL: iopscience.iop.org/issue/1674.
Gan, W.Q., Zhu, C., Deng, Y.Y., Li, H., Su, Y., Zhang, H.Y., et al.: 2019c, Advanced Space-based Solar Observatory (ASO-S): an overview. *Res. Astron. Astrophys.* **19**, 156. DOI. ADS.
Huang, Y., Li, H., Gan, W.Q., Li, Y.P., Su, J.T., Deng, Y.Y., et al.: 2019, The Science Operations and Data Center (SODC) of the ASO-S mission. *Res. Astron. Astrophys.* **19**, 163. DOI. ADS.
Kosugi, T., Makishima, K., Murakami, T., Sakao, T., Dotani, T., Inda, M., et al.: 1991, The Hard X-ray Telescope (HXT) for the SOLAR-A mission. *Solar Phys.* **136**, 17. DOI. ADS.
Kuhn, J.R., Lin, H., Loranz, D.: 1991, Gain calibrating nonuniform image-array data using only the image data. *Publ. Astron. Soc. Pac.* **103**, 1097. DOI. ADS.
Lemen, J.R., Title, A.M., Akin, D.J., Boerner, P.F., Chou, C., Drake, J.F., et al.: 2012, The Atmospheric Imaging Assembly (AIA) on the Solar Dynamics Observatory (SDO). *Solar Phys.* **275**, 17. DOI. ADS.
Li, H., Chen, B., Feng, L., Li, Y., Huang, Y., Li, J.W., et al.: 2019, The Lyman-alpha Solar Telescope (LST) for the ASO-S mission—I. Scientific objectives and overview. *Res. Astron. Astrophys.* **19**, 158. DOI. ADS.
Li, J.W., Li, H., Li, Y., Feng, L., Huang, Y., Zhao, J., et al.: 2021, Methodology for in-flight flat-field calibration of the Lyman-alpha Solar Telescope (LST). *Res. Astron. Astrophys.* **21**, 121. DOI. ADS.
Liu, W., Zhang, Z., Wu, J., Ma, T., Zhang, Y., Hu, Y.M., et al.: 2022, Pre-launch characterization of the spectrometer of Hard X-ray Imager (HXI) onboard the ASO-S mission. *J. Instrum.* **17**, P05045. DOI. ADS.
Pesnell, W.D., Thompson, B.J., Chamberlin, P.C.: 2012, The Solar Dynamics Observatory (SDO). *Solar Phys.* **275**, 3. DOI. ADS.
Scherrer, P.H., Schou, J., Bush, R.I., Kosovichev, A.G., Bogart, R.S., Hoekseme, J.T., et al.: 2012, Design and ground calibration of the Helioseismic and Magnetic Imager (HMI) instrument on the Solar Dynamics Observatory (SDO). *Solar Phys.* **275**, 207. DOI. ADS.
Su, J.T., Bai, X.Y., Chen, J., Guo, J.J., Liu, S., Wang, X.F., et al.: 2019a, Data reduction and calibration of the FMG onboard ASO-S. *Res. Astron. Astrophys.* **19**, 161. DOI. ADS.
Su, Y., Liu, W., Li, Y.P., Zhang, Z., Hurford, G.J., Chen, W., et al.: 2019b, Simulations and software development for the Hard X-ray Imager onboard ASO-S. *Res. Astron. Astrophys.* **19**, 163. DOI. ADS.
Wan, Q., Zhang, Y., Guo, J.H., Zhang, Y.Q., Xu, X.: 2022, Design of front-end electronics for HXI spectrometer flight model on-board ASO-S satellite. *J. Instrum.* **17**, P02020. DOI. ADS.
Zhang, Y., Guo, J.H., Zhang, Z., Chen, D.Y., Hu, Y.M., Zhang, Y.Q., Ma, T., Huang, Y.Y.: 2019a, Spectrometer of hard X-ray imager payload onboard the ASO-S mission. *Nucl. Sci. Tech.* **30**, 1. DOI.
Zhang, Z., Chen, D.Y., Wu, J., Chang, J., Hu, Y.M., Su, Y., et al.: 2019b, Hard X-ray Imager (HXI) onboard the ASO-S mission. *Res. Astron. Astrophys.* **19**, 160. DOI. ADS.

Authors and Affiliations

Weiqun Gan[1] · Cheng Zhu[2] · Yuanyong Deng[3] · Zhe Zhang[1] · Bo Chen[4] · Yu Huang[1] · Lei Deng[2] · Haiyan Wu[5] · Haiying Zhang[6] · Hui Li[1] · Yang Su[1] · Jiangtao Su[3] · Li Feng[1] · Jian Wu[1] · Jijun Cui[5] · Chi Wang[5] · Jin Chang[1] · Zengshan Yin[2] · Weiming Xiong[5] · Bin Chen[5] · Jianfeng Yang[7] · Fu Li[7] · Jiaben Lin[3] · Junfeng Hou[3] · Xianyong Bai[3] · Dengyi Chen[1] · Yan Zhang[1] · Yiming Hu[1] · Yaoming Liang[5] · Jianping Wang[2] · Kefei Song[4] · Quanfeng Guo[4] · Lingping He[4] · Guang Zhang[4] · Peng Wang[4] · Haicao Bao[2] · Caixia Cao[2] · Yanping Bai[2] · Binglong Chen[2] · Tao He[2] · Xinyu Li[2] · Ye Zhang[2] · Xing Liao[2] · Hu Jiang[2] · Youping Li[1] · Yingna Su[1] · Shijun Lei[1] · Wei Chen[1] · Ying Li[1] · Jie Zhao[1] · Jingwei Li[1] · Yunyi Ge[1] · Ziming Zou[5] · Tai Hu[5] · Miao Su[5] · Haidong Ji[8] · Mei Gu[9] · Yonghuang Zheng[10] · Dezhen Xu[11] · Xing Wang[12]

✉ W. Gan
wqgan@pmo.ac.cn

1 Key Laboratory of Dark Matter and Space Astronomy, Purple Mountain Observatory, Chinese Academy of Sciences, Nanjing 210023, China

2 Innovation Academy for Microsatellites, Chinese Academy of Sciences, Shanghai 201203, China

3 National Astronomical Observatories, Chinese Academy of Sciences, Beijing 100101, China

4 Changchun Institute of Optics, Fine Mechanics and Physics, Chinese Academy of Sciences, Changchun 130033, China

5 National Space Science Center, Chinese Academy of Sciences, Beijing 100190, China

6 Nanjing Institute of Astronomical Optics & Technology, National Astronomical Observatories, Chinese Academy of Sciences, Nanjing 210042, China

7 Xi'an Institute of Optics and Precision Mechanics, Chinese Academy of Sciences, Xi'an 710119, China

8 Aerospace System Engineering, Shanghai 201109, China

9 Beijing Special Engineering and Design Institute, Beijing 100028, China

10 Jiuquan Satellite Launch Center, Jiuquan 732750, China

11 Beijing Institute of Tracking and Telecommunications Technology, Beijing 100094, China

12 State Key Laboratory of Astronautic Dynamics, Xi'an 710043, China